Sevenfold Coordinated MgSe: Experimental Internal Atom Position Determination to 146 GPa, Diffraction Studies to 202 GPa, and Theoretical Studies to 500 GPa

Arthur L. Ruoff, Ting Li, Allen C. Ho, Min-Fan Pai, Huan Luo, Ray G. Greene, and Chandrabhas Narayana
Department of Materials Science And Engineering, Cornell University, Ithaca, New York 14853

Jay C. Molstad, Steven S. Trail, and Francis J. DiSalvo, Jr.
Department of Chemistry, Cornell University, Ithaca, New York 14853

P. E. van Camp
Department of Physics, University of Antwerpen Groenenborggklaan, 171, B-2000, Antwerpen, Belgium
(Received 14 October 1997)

MgSe has been studied using energy dispersive x-ray diffraction to 202 GPa and local density approximation and ultrasoft pseudopotentials to 500 GPa. MgSe undergoes a "continuous" phase transformation from the rocksalt to FeSi ($B28$) beginning at around 99 ± 8 GPa and approaching sevenfold coordination at 202 GPa. Theoretical computation finds the $B28$ transition beginning at 58 GPa followed by a transition to an orthorhombic distortion of the $B2$ structure at 429 GPa. [S0031-9007(98)07261-5]

PACS numbers: 64.70.Kb, 61.10.–i, 62.50.+p, 64.30.+t

The chalcogenides of Ba, Sr, and Ca have the sixfold coordinated NaCl structure ($B1$) and transform at high pressure to the eightfold coordinated CsCl structure ($B2$) except for BaO which transforms to a distorted CsCl structure [1]. The compounds of MgSe, MgS, and MgO also have the $B1$ structure. MgO is of great interest to geophysicists as it is one likely component of the lower mantle [2]. It has been calculated that there will be a $B1 \rightarrow$ cesium chloride ($B2$) structure transformation at around 600 GPa for MgO [3,4] and at 231 GPa for MgS [5]. From an empirical map based on the ratio of the cation radius to the anion radius versus the logarithm of the pressure of the chalcogenides of Ba, Sr, and Ca, the $B1$ to $B2$ transformation is expected as follows: MgSe (175 GPa), MgS (172 GPa), MgO (210 GPa), if no other transition intervenes [1].

The MgSe powder sample was prepared from the reaction of Mg shavings (Strem Chemicals 99.9%) and selenium pieces (Aldrich 99.9%), placed in a boron nitride crucible, then evacuated and sealed in a quartz tube and heated at 1023 K for 24 hours. The x-ray powder diffraction of the sample showed it to be single phase, with a cubic cell with $a = 5.466$ Å; the literature value is $a = 5.462$ Å. The samples were handled in a dry argon environment to avoid exposure to air. The first experiment used gold [6] as a pressure marker and reached 60 GPa. The second experiment used platinum [7] as a pressure marker and reached 146 GPa. Data were collected on downloading to 109 GPa with no hysteresis. The equation of state (EOS) was determined from these two experiments. In the third experiment which reached 202 GPa the pressure was determined from the EOS of MgSe so that pressure marker peaks did not obfuscate the x-ray pattern. In the last experiment, the diamond anvil cell (DAC) was rotated about the x-ray beam, clockwise and anticlockwise by 360°, alternately, while the experiment was in progress, in an effort to reduce the effect of texturing in the sample. No pressure medium was used in any of these experiments.

Energy dispersive x-ray diffraction (EDXD) experiments were performed at the Cornell High Energy Synchrotron Source (CHESS) to get the x-ray diffraction spectra and EOS of the MgSe sample [8]. A set of tungsten apertures collimated the incident x-ray beam to 20×20 μm^2 in the first two experiments, and 17×17 μm^2 in the third experiment. The diffraction geometry was calibrated with gold foil. The typical collection times for a spectrum were approximately 20 minutes in the first experiment, 60 minutes in the second experiment, and around 1 to 2 hours in the third experiment. On loading from 0 to 96 GPa all spectra indexed well to the initial $B1$ phase. Figure 1(a) shows a typical EDXD spectrum of MgSe near 35 GPa indexed to the $B1$ structure [9]. For pressures greater than 96 GPa, new sample diffraction lines appear in addition to those of the rocksalt pattern, indicating a phase transition. Figure 1(b) shows an EDXD spectrum of MgSe at 99 GPa with arrows pointing out the extra peaks. The intensities of the new peaks increased gradually with pressure. It was found that a simple cubic lattice with the same lattice constant as that of the rocksalt phase produces all the interplanar spacings of the observed peaks. An excellent fit (of the 32 data points to 146 GPa) exists with the two-parameter EOS of Birch [10]

$$P = (3/2)B_0(x^{7/3} - x^{5/3}) \times [1 + (3/4)(B_0' - 4)(x^{2/3} - 1)], \quad (1)$$

where $x = V_0/V$, B_0 is the isothermal bulk modulus at zero pressure, and B_0' is the pressure derivative of the isothermal bulk modulus evaluated at zero pressure. The resulting values of the two parameters, applicable to

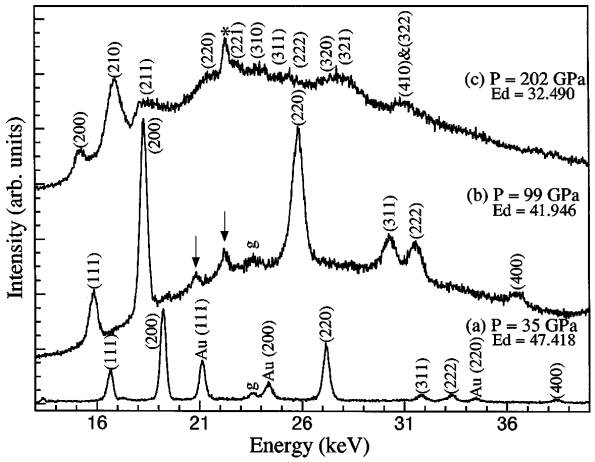

FIG. 1. EDXD diffraction spectra of MgSe. g is gasket; Au is gold; all other labeled peaks are the sample. Ed is in the unit of keV Å. (a) Original $B1$ structure near 35 GPa. (b) 99 GPa, new peaks shown with arrows. (c) 202 GPa, showing $B28$ phase. In (b) and (c) pressure was determined from the measured lattice parameter of MgSe and its EOS, and also the sample was rotated about the x-ray beam (see text). The $*$ in curve (c) may represent the disallowed diamond peak (112) since it would come from the highly strained tip region of the diamond. We note that this peak and four other peaks from diamond at energies above 45 keV are all very much sharper than the peaks from MgSe. These five peaks give $a = 3.573 \pm 0.002$ Å. We do not rule out the possibility that the $*$ peak in curve (c) is a new peak of a second phase.

TABLE I. List of the observed interplanar spacings (d) and relative intensities (I)* of MgSe at 146 GPa along with the theoretical corresponding values based on the FeSi structure. The fitted lattice parameter is 4.450 ± 0.002. The energy-interplanar spacing product was $Ed = 42.590$ keV Å.

(hkl)	d_{obs} (Å)	d_{calc} (Å)	I_{obs} (%)	I_{calc} (%)
(110)	3.143	3.147	3	9
(111)	2.576	2.569	38	49
(200)	2.224	2.225	100	100
(210)	1.991	1.990	64	64
(211)	1.813	1.817	12	12
(220)	1.578	1.573	28	38
(221)	1.485	1.483	20	25
(310)	1.408	1.407	9	7
(311)	1.342	1.342	7	6
(222)	1.288	1.285	18	6
(321)	1.190	1.189	14	10
(410) + (322)	1.081	1.079	3	9
(421)	0.974	0.971	2	5

*The $(h00)$ peaks, for odd values of h, of $B28$ always have $I = 0$. R_B is based on all the peaks from (110) to (521) including those of zero observed intensities. The minimum is at $u = 0.048 \pm 0.003$ and $w = 0.452 \pm 0.003$ with $R_B = 0.24$. In other patterns at different pressures the following peaks were also present: (320), (400), (331), (420), (332), (422), (510), (511), (423), and (521).

both phases, are $B_0 = 62.8 \pm 1.6$ GPa and $B_0' = 4.1 \pm 0.1$ with $V_0(B28) = V_0(B1)$. The $B28$ structure [11,12] was assigned to the high pressure phase; the magnesium atoms are located at $u\ u\ u$; $u + 1/2, 1/2 - u, \bar{u}$; $\bar{u}, u + 1/2, 1/2 - u$; $1/2 - u, \bar{u}, u + 1/2$ and selenium atoms at $w\ w\ w$; $w + 1/2, 1/2 - w, \bar{w}$; $\bar{w}, w + 1/2, 1/2 - w$; $1/2 - w, \bar{w}, w + 1/2$ [12]. If $u = 0$ and $w = 1/2$, this is the NaCl ($B1$) structure. The experimental values of u and w are obtained by minimization of the Bragg R_B. See Table I. Here $R_B = (\sum I_{\text{obs}} - I_{\text{calc}})/\sum I_{\text{obs}}$ (see Table 1.3 of Ref. [13]). At 146 GPa, there is a sharp minimum at $u = 0.0481$, $w = 0.4520$.

As texturing was evident in the first two experiments, a third experiment was performed in which the pressure vessel and hence the sample were rotated about the x-ray beam to average (partially) the effect of texturing. This is similar to the use of image plates in angle dispersive x-ray diffraction (ADXD). It plays the same role as does averaging over 360° in a Debye Scherrer ring on an image plate in ADXD [14]. The diamond tips used had (100) faces. When the cell is rotated single crystal peaks from the diamond can occur. At the angles used no allowed diamond peaks existed below 45 keV. However, allowed peaks were seen above 45 keV. Figure 1(c) shows a diffraction pattern at 202 GPa. At 170 GPa and above, the (210) peak is the strongest peak. Figure 2 shows experimental data at 146 GPa and the calculated peaks. The background intensity at a specific pressure as a function of energy E was fitted to the expression

$$I_B(E) = \alpha\ \exp[-(\beta/E^3 - \gamma/E^4)]\ \exp(-\delta E), \quad (2)$$

and this was subtracted from the total intensity to give the corrected pattern. The peaks were fitted with Gaussians, to obtain peak positions (and hence the interplanar spacing) and the FWHM's. The theoretical relative intensity pattern for a case where the 200 peak is strongest was calculated for the sum of all the theoretical peaks

$$(I_{hkl}/I_{200}) = [I_B(hkl)M_{hkl}F_{hkl}^2\mathcal{I}_{200}E_{200}^2]/[I_B(200)M_{200}F_{200}^2\mathcal{I}_{hkl}E_{hkl}^2], \quad (3)$$

where M is multiplicity, F is the cell scattering factor, and $\mathcal{I}$ is due to the incoherent Compton scattering from the diamond.

At 202 GPa there is a sharp minimum at $u = 0.0828$ and $w = 0.4173$, which we round off to 0.08 ± 0.01 and 0.42 ± 0.01. This corresponds to six atoms at $0.53a \pm 0.01a$ and one at $0.58a \pm 0.01a$. The theoretical values at 202 GPa are $u = 0.0759$ and $w = 0.4136$ (see Fig. 3). For seven equidistant neighbors $u = 0.095\,495$ and $w = 0.404\,508$, the bond distance is $0.5352a$, and $w = 1/2 - u$.

The calculations were performed in the framework of the local density approximation using ultrasoft pseudopotentials [15] and a large plane wave basis. For the exchange-correlation part the authors used the Ceperley-Alder expression [16] as parametrized by Perdew and

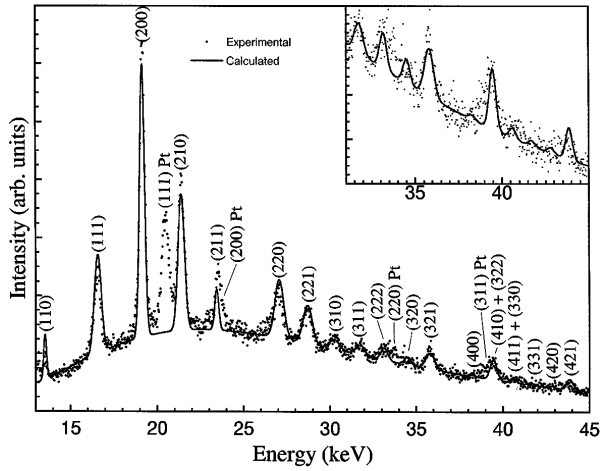

FIG. 2. Experimental and theoretical x-ray patterns (based on minimization of R_B with respect to u and w) for the $B28$ structure of MgSe at 146 GPa. The inset shows amplified intensities from 31 to 45 keV and the two energy axes coincide. A peak position in the inset is at the same energy as in the main figure.

Zunger [17]. The optimization of the internal parameters and of the lattice parameters was performed with the Broyden-Fletcher-Goldfarb-Shanno algorithm [17]. The calculated total energies were then fitted to the two-parameter Birch EOS from which the bulk modulus and its pressure derivative were determined. The main difference from previous work [18] is that now the core radii were taken a lot smaller so that calculations can be performed to higher pressures. Moreover, a larger cutoff of 64 Ry was used and more structures were considered, e.g., rocksalt ($B1$), cesium chloride ($B2$), zinc blende ($B3$), wurtzite ($B4$), nickel arsenide ($B8$), iron silicide ($B28$), and simple tetragonal (ST2) and orthorhombic (SO2) structures [19]. SO2 is a distortion of ST2, which in turn is a distortion of $B2$. Table II shows the lattice constant, bulk modulus, and its pressure derivative for five structures. Table III shows the calculated transition pressures, the volume change at the transitions, and the energy difference between the two structures at the transitions. For the SO2 structure at the transition pressure (429.3 GPa) we find a b/a value slightly smaller than 1 and a c/a value slightly larger than 1. Thus SO2 is a slightly distorted CsCl structure. It is always more stable than $B2$, at high pressure. It is possible that thermal effects not considered here would make the more symmetrical CsCl structure the stable high pressure phase at room temperature. Were the ST2 and SO2 structure absent, a $B28$ to $B2$ equilibrium transition point would exist at 472 GPa while if $B28$ were also absent the $B1$ to $B2$ transition would be at 170 GPa.

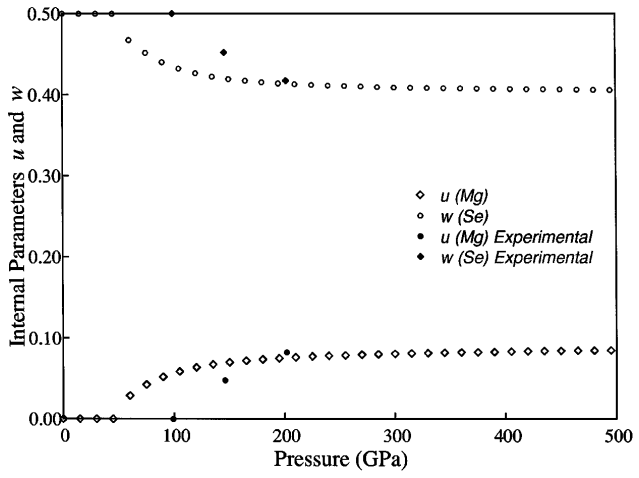

FIG. 3. Calculated internal atomic positions of u of Mg and w of Se as a function of pressure and experimental values at 99, 146, and 202 GPa. The data at 202 GPa have a larger error bar than the other two points.

TABLE II. Calculated lattice constant a, bulk modulus B_0, and its pressure derivative B_0' for five phases of MgSe, namely, rocksalt ($B1$), cesium chloride ($B2$), iron silicide ($B28$), simple tetragonal (ST2), and simple orthorhombic (SO2).

	$B1$	$B2$	$B28$	ST2	SO2
a	5.4975	3.4413	5.4967	3.4133[a]	3.4133[a]
B_0	68.12	63.68	51.11	60.79	61.55
B_0'	4.08	4.04	4.10	4.08	4.07

[a]These structures tranform to $B2$ at $P = 0$.

Finally, a comparison of the experimental and theoretical results is made. Using the Birch EOS, the experimental values of $B_0 = 62.8$ GPa and $B_0' = 4.1$ agree fairly well with the calculated values of 68.12 GPa and 4.08, respectively. Experimentally it was found, at a pressure of 202 GPa, that the internal atomic positions $u = 0.08$ and $w = 0.42$ are near the theoretically calculated values of 0.0759 and 0.4136, respectively. At 202 GPa, MgSe is close to the sevenfold structure as in AuBe.

The present experimental determination was limited by broad peak widths owing to strain broadening and pressure gradients (caused by the large yield stress; for comparison MgO has a yield strength of at least 11 GPa at 227 GPa [20]). Thus, in the earliest stages of the transformation because of the presence of a pressure gradient and a finite beam size, the diffraction pattern would be partially from the $B1$ phase and partially from the $B28$ phase. This would be followed by a stage in which only $B28$ was present but with a large variation of u and w across the finite beam since these vary rapidly near the transition pressure. In future experiments, to determine u and w in the range in which their variation with pressure

TABLE III. Calculated transition pressure P (in GPa), the volume change ΔV (in %), and the energy difference ΔE (in meV) for the phase transition from $B1$ to $B28$ and $B28$ to SO2.

	$B1$ to $B28$	$B28$ to SO2
P	57.0	429.3
ΔV	1.5	1.2
ΔE	74.0	245.9

is large, a hydrostatic medium, such as helium, should be used to minimize these effects. We intend to carry out such studies. If broadening occurring during the transformation is small, then the intrinsic detector peak width of $0.145\sqrt{E(\mathrm{keV})/5}$ would apply. Should this prove to be a limitation, then the detector needs to be replaced with one of much higher resolution such as the microcalorimeter (bolometer) detectors which are undergoing rapid development [21]. With near hydrostatic pressure, and sensitive detectors, and possibly with sample rotation, EDXD has a bright future as a tool for structural determination including accurate determination of internal atom positions.

Within our experimental error limits there is no noticeable volume change in the $B1$ to $B28$ transition, so it is likely that the transformation is second order (although theoretical calculations show a small volume change). Based on symmetry arguments, the X_5^- irreducible representation can drive such a transition from $Fm\bar{3}m$ (225) to T^4P2_13 (198) [22]. Another fact that gives some reinforcement to this conclusion is that the reverse transformation during unloading proceeded without any observable hysteresis.

The distorted rocksalt structure discovered in MgSe at around one megabar is the first example of a sixfold coordinated rocksalt structure transforming to a sevenfold coordinated iron silicide structure at high pressure. It is interesting to note that FeSi is a narrow gap semiconductor at low temperature [23] and becomes metallic over 300 K [24], which is consistent with the expected metallization of MgSe at high pressure. It would be instructive to consider $B28$ as a possible structure in theoretical calculations for MgS and MgO as well. The potential significance of the $B28$ structure lies in the conjecture that if the $B28$ structure has a substantially lower transition pressure when compared to $B2$ for MgO, it will have important geological implications [20].

We thank the CHESS staff for their technical assistance and the National Science Foundation for support of this research through Grant No. DMR 9530634.

[1] C. Narayana, V. J. Nesamony, and A. L. Ruoff, Phys. Rev. B **56**, 14 338 (1997).
[2] F. Birch, J. Geophys. Res. **57**, 227 (1952).
[3] K. J. Chang and M. L. Cohen, Phys. Rev. B **30**, 4774 (1984).
[4] M. D. Jackson and R. G. Gordon, Phys. Rev. B **38**, 5654 (1988).
[5] P. E. van Camp, V. E. van Doren, and J. L. Martins, Phys. Status Solidi B **190**, 193 (1995).
[6] J. C. Jamieson, J. Fritz, and M. H. Manghnani, Adv. Earth Planet. Sci. **12**, 27 (1980).
[7] N. C. Holmes, J. A. Moriarty, G. R. Gathers, and W. J. Nellis, J. Appl. Phys. **66**, 2962 (1989).
[8] M. Baublitz, Jr., V. Arnold, and A. L. Ruoff, Rev. Sci. Instrum. **52**, 1616 (1981).
[9] C. Narayana, A. C. Ho, M-F. Pai, and A. L. Ruoff, in Review of High Pressure Science and Technology, edited by M. Nakahara (to be published).
[10] F. Birch, J. Geophys. Res. **83**, 1257 (1978).
[11] L. Pauling and A. M. Soldate, Acta. Crystallogr. **1**, 212 (1948).
[12] B. D. Cullity, Trans. AIME **171**, 396 (1947).
[13] R. A. Young, *The Rietveld Method* (Oxford University Press, New York, 1993), p. 22.
[14] Y. Fujii, K. Hose, Y. Ohishi, N. Hamaya, K. Takemura, O. Shimomura, T. Kigegawa, Y. Amemiya, and T. Matushita, Phys. Rev. Lett. **63**, 536 (1989).
[15] N. Troullier and J. L. Martins, Solid State Commun. **74**, 613 (1990); Phys. Rev. B **43**, 1993 (1991).
[16] D. Ceperley and B. Alder, Phys. Rev. Lett. **45**, 566 (1980).
[17] J. P. Perdew and A. Zunger, Phys. Rev. B **23**, 5048 (1981).
[18] J. Olsen and P. Jorgensen, J. Chem. Phys. **77**, 6109 (1982).
[19] P. E. van Camp, V. E. van Doren, and J. L. Martins, Phys. Rev. B **55**, 775 (1997).
[20] T. S. Duffy, R. J. Hemley, and H-K. Mao, Phys. Rev. Lett. **74**, 1371 (1995).
[21] D. A. Wollman, G. C. Hilton, K. D. Irwin, and J. Martins, in *Proceedings of Microscopy and Microanalysis*, edited by G. N. Bailey, J. M. Corbett, R. V. W. Dimlich, J. R. Michael, and N. J. Zaluzec (San Francisco Press, San Francisco, 1996), p. 488.
[22] H. T. Stokes and D. M. Hatch, *Isotropy Subgroups of the 230 Crystallographic Space Groups* (World Scientific, Teanech, NJ, 1988).
[23] V. Jaccarino, G. K. Wertheim, J. H. Wernick, L. R. Walker, and S. Arajs, Phys. Rev. **160**, 476 (1967).
[24] R. Wolfe, J. H. Wernick, and S. E. Haszko, Phys. Lett. **19**, 449 (1965).